IEEE Access
Multidisciplinary | Rapid Review | Open Access Journal

Received April 12, 2021, accepted May 12, 2021, date of publication May 26, 2021, date of current version June 7, 2021.

Digital Object Identifier 10.1109/ACCESS.2021.3083544

An Improved Fault Diagnosis Strategy for Process Monitoring Using Reconstruction Based Contributions

HAJER LAHDHIRI[1], AHAMED ALJUHANI[2], KHAOULA BEN ABDELLAFOU[3], AND OKBA TAOUALI[1,2]

[1]National Engineering School of Monastir, University of Monastir, Monastir 5000, Tunisia
[2]Department of Computer Engineering, Faculty of Computers and Information Technology, University of Tabuk, Tabuk 47512, Saudi Arabia
[3]Department of Computer Science, Faculty of Computers and Information Technology, University of Tabuk, Tabuk 47512, Saudi Arabia

Corresponding author: Okba Taouali (taoualiok@gmail.com)

ABSTRACT Air pollution has become the fourth leading cause of premature death on Earth. Air pollution causes poor health and death; about one case out of every ten deaths worldwide is caused by air pollution, which is six times more than malaria. Human activities are the main cause of air pollution, such as chemical industries, road traffic, and fossil fuel power plants. Over the span of several years, monitoring air quality has become an exigent and essential task. In order to limit the health impact of air pollution and to ensure safe operation of chemical processes, it is necessary to quickly detect and locate instrumentation defects. There are several process monitoring techniques in the literature. Among these techniques is the one selected for this work for the detection and location of sensor faults: the kernel principal component analysis (KPCA) method, which was selected for its primary advantages of easy employment and less necessity for prior knowledge. Using the KPCA method for monitoring nonlinear systems, the calculation cost and the memory size are related to the number of initial data. This is currently a major limitation of the KPCA method, especially in industrial environments. In order to remedy this limitation, in this paper we propose a new method of detection and localization. The key idea of this approach is to extend the method of localization based on the principle of reconstruction-based contributions (RBC) by downsizing the kernel matrix in the characteristic space. The proposed technique is named reconstruction-based contribution reduced rank kernel principal component analysis(RBC-RRKPCA). The approach is demonstrated using real air quality monitoring network data and simulated data from the Tennessee Eastman process (TEP) as a challenging benchmark problem. We also present a comparative study of the performances of the conventional diagnostic technique RBC-KPCA and the proposed technique RBC-RRKPCA. The results in this paper reveal that the proposed technique achieves the highest detection and localization accuracy.

INDEX TERMS Quality, fault detection, fault isolation, KPCA, nonlinear process monitoring, RBC, RRKPCA, Tennessee Eastman process (TEP).

I. INTRODUCTION

The purpose of the chemical industry is to change the chemical structure of natural materials in order to derive products that are useful in other industries or in everyday life. Chemicals are obtained from raw materials—mainly minerals, metals, and hydrocarbons—in a series of processing steps. Anytime processes that use temperature and pressure are used to change molecular structure or create new products from chemical compounds, there is a risk of fire, explosion, or emission of liquids, vapors, gases, and toxic substances that cause air pollution.

Air pollution has significant effects on health and the environment. Air pollution is currently the first environmental concern of the French. Natural phenomena, but especially human activities, are the source of pollutant emissions in the form of gases or particles into the atmosphere. Once released into the air, these substances are transported under the impact of wind, rain, and temperature gradients in the atmosphere—sometimes up to thousands of kilometers from the source of

The associate editor coordinating the review of this manuscript and approving it for publication was Qingchao Jiang.

emission. They can also undergo transformations from chemical reactions under the influences of certain meteorological conditions (heat, light, humidity, etc.) and from reactions in the air between these substances. This results in the appearance of other pollutants. The most well-known health effects of air pollution are those on the respiratory and cardiovascular systems (cerebrovascular accidents, heart disease, etc.).

The quality of the air we breathe is determined by the concentrations of different pollutants, which are most often expressed in micrograms per cubic meter of air (μg/m3). Over the last fifteen years, four pollutants have been mainly monitored: sulfur dioxide (SO2), nitrogen dioxide (NO2), ozone (O3), and particulate matter (PM10). The concentrations of these pollutants are measured at different points in the French territory, mainly in a situation of urban bottom, making it possible to evaluate the exposure of the population to the atmospheric pollution of bottom or proximity to urban centers.

Currently, monitoring of air pollution (measuring stations and modeling) has been described in the literature [1], [2] as ensuring that air quality standards and preventative measures minimize the harmful effects of changing many pollutants. The objective of the air monitoring program is to monitor and characterize the impact of air pollution through retrospective analyses based on methods of control for potential confounders. It also carries out quantitative assessments of the health impact of air pollution at the national and local levels, which make it possible to simulate the effects of new developments or actions to reduce emissions and, thus, guide the choice of decision makers. At certain times of the year, especially in winter, spring, and summer, there are peaks (or episodes) of pollution in the metropolitan territory. A spike (or episode) is when air pollution exceeds or is at risk of exceeding the information and recommendation threshold (or alert threshold) defined by the national regulations for the four pollutants.

Chemical processes are a major source of air pollution. Therefore, rapid validation, detection, and diagnosis of measurement errors is a crucial step in guaranteeing safe and optimal operations in chemical processes. In these tasks, several data-driven fault detection methods have been developed in the literature to detect sensor errors or unnatural changes in main measured air quality parameters [3], [4], [1] and chemical processes such as the Tennessee Eastman process (TEP) [5]–[7]. In data-driven modeling [8], machine learning algorithms such as artificial neural networks (ANNs) and support vector machines (SVMs) [9]; multivariate statistical approaches such as kernel partial least squares (KPLS) [10] and kernel principal component analysis (KPCA) [11]; and logical analysis of data (LAD) [12] are machine learning approaches that are used to discover the hidden knowledge in historical data. KPCA and KPLS are widely used to detect and diagnose faults in the controlled TEP [13] and in the air quality monitoring network. In [14], the authors propose a new defect detection technique that merges the generalized likelihood ratio test (GLRT) and exponentially weighted moving average (EWMA). Recently, in [15], a new defect detection technique based on the reduced kernel partial least squares (RKPLS) method was proposed to anticipate the concentrations of various pollutants and to aid in understanding variations in air quality networks.

After fault detection, it is important to identify the process variables associated with the fault. Indeed, fault identification is described as the capability of the monitoring process to be able to discover the origin of the fault. In general, the fault identification approach depends on the detection procedure implemented. In the literature, many principal component analysis (PCA)-based approaches have been proposed, such as the fault localization method using residue structuring [16]. In 1999, [17] proposed a new method called partial PCA. Indeed, this approach is defined as an extension of the residue structuring approach and has been successfully validated [3], [18]. In [19] and [20], the authors proposed an extension of these methods for fault diagnosis in dynamic nonlinear systems. The main idea of these methods is to create a set of partial models so that each model is affected by a subset of defects.

Another approach to fault localization by PCA is the contribution diagrams approach [21]–[23]. The contributions are actually the effects of the defect on the observed measurement vector [24], [25]. They are based on the idea that variables with large contributions to a default detection index are probably the cause of default. However, even for simple sensor faults, contribution diagrams do not guarantee a correct diagnosis. As an alternative to contribution diagrams, [13] proposed a method for calculating contributions based on the reconstruction of the defect detection index along the direction of a variable. Reconstructing a defect detection index along a variable direction minimizes the effect of this variable on the detection index. Thus, the amount of reconstruction in one direction of a variable can be used as the amount of contribution of the variable to the defect detection index that is reconstructed. Therefore, this amount of reconstruction will be referred to as the reconstruction-based contribution (RBC) of this variable to the default detection index. This approach has been developed for the identification of linear process defects with the PCA technique. In order to show that the RBC method is better than the contribution calculation method, a rigorous analysis of the diagnostic ability is provided for the traditional contribution calculation method and the RBC method. There is evidence that the RBC method ensures correct fault location and that the incriminated variable has the largest RBC for the case of random error amplitudes. These results are generally applicable for the Squared Prediction Error (SPE) index, Hotteling's T2 index, and the combined indexes [26] and [27]. The RBC method depends on the identification of defects by reconstruction, but it does not require knowledge of fault directions. However, fault diagnosis for nonlinear systems cannot be done with contribution diagrams because there seems to be no way to calculate them with KPCA. Due to the nonlinear transformation used (which is not explicit), the estimate of

the magnitude of the defects cannot be performed in the characteristic space. To have a valid result, it is necessary to reconstruct the transformed data in the input space; however, this reverse return operation is called the pre-image problem. The solution to this problem is to solve an optimization problem, because there is no exact solution and, even if it exists, it cannot be unique. In 2010, [28] proposed RBC for the kernel PCA (RBC-KPCA). In [29], the convergence of the optimization algorithm is not guaranteed with the Hotteling T2 index, so RBCs with KPCA are only calculated with the SPE index and the combined indexes. Nevertheless, the convergence time of the optimization algorithm increases if the dimension of the kernel matrix is important.

To overcome this problem, we have proposed in this article a new fault diagnosis technique, which combines the benefits of the reduced rank KPCA technique and the principle of RBC. The proposed technique, RBC-RRKPCA, ameliorates the detection and localization performances compared to conventional RBC-KPCA. The principle of the RBC-RRKPCA is first to construct the reduced reference model by using RRKPCA, and second to use the SPE index and the principle of RBC for detection and localization purposes. The key objective of this paper is to prove the application of the proposed technique for fault diagnosis using real air quality monitoring network data and simulated TEP data.

The rest of the paper is organized as follows. In Section II, a review of KPCA and RRKPCA methods is presented. In Section III, we present the suggested RBC-RRKPCA method and its mathematical formulation. Section IV demonstrates the effectiveness of the developed fault diagnosis approach using real air quality monitoring network data and simulated TEP data. Conclusions are given at the end of the paper.

II. FAULT DETECTION METHODS

A. NOTATIONS

In the Table 1, all notations are presented.

TABLE 1. Notations.

K_r : Reduced kernel matrix	ξ_i : fault direction
Λ_r : Eigenvalues matrix of the reduced kernel matrix	RBC_i : the amount of reconstruction in the direction ξ_i
V_r : Eigenvectors matrix of the reduced kernel matrix	f_i : default amplitude
m : Number of system variables	z_i^r : reconstructed observation
N : Number of samples	
ℓ : Number of selected principal components	
r : Number of reduced of samples	
X_r : The reduced data matrix	
δ_α^2 : the control limit of the SPE index	

B. REVIEW OF KPCA METHOD

The KPCA method is a simple and interesting technique developed by Schölkopf *et al.* [30] to model faithfully the non-linear relationships between process data. Using kernel function [31], KPCA can ably project input data with a linearly inseparable structure over a higher dimensional space in which data can be linearly separated. Compared to other nonlinear extensions of PCA [32], [33], the KPCA method only needs to solve an eigenvalue problem without any nonlinear optimization.

The characteristic space **H** is transformed non-linearly from the original space **E** using a nonlinear projection function ϕ. Let the sample $x \in \mathrm{E}$, its projection in the characteristic space **H** via the function ϕ can be defined as:

$$\begin{aligned} \phi : \mathrm{E} \subset \mathbb{R}^m &\rightarrow \mathrm{H} \subset \mathbb{R}^h \\ x &\rightarrow \phi(x) \end{aligned} \tag{1}$$

Let $X = [x_1, \ldots, x_i, \ldots, x_N]^T$ the normalized input data matrix.

Where $x \in E \subset R^m$ is an input data vector, where m presents the process variables number and N presents the samples number. The implicit KPCA model can be given by the Eigen- values decomposition of the covariance matrix C_Φ, which is given by:

$$C_\Phi = \frac{1}{N} \sum_{i=1}^{N} \phi(x_i)\, \phi(x_i)^T \tag{2}$$

Let $\chi = [\phi(x_1) \ldots \phi(x_i) \ldots \phi(x_N)]^T \in \mathbb{R}^{N \times h}$ defines the matrix of data in the characteristic space **H**, so the covariance matrix C_Φ can be expressed as follows:

$$C_\Phi = \frac{1}{N} \chi^T \chi \tag{3}$$

The principal components of the projected data in the characteristic space are calculated by solving the decomposition into eigenvalues and eigenvectors of the matrix C_Φ such that:

$$\lambda_j \mu_j = C_\Phi \mu_j; \quad j = 1, \ldots, h \tag{4}$$

With μ_j is the j^{th} eigenvector and λ_j is the j^{th} eigenvalue associated. For $\lambda_j \neq 0$, it exists $\alpha_{i,j}; i = 1 \ldots N$ coefficients such that all eigenvectors μ_j may be considered as a linear combination of $[\phi(x_1) \ldots \phi(x_i) \ldots \phi(x_N)]$ and can be defined by:

$$\mu_j = \sum_{i=1}^{N} \alpha_{i,j}\, \phi(x_i) \tag{5}$$

However, the projection function ϕ is not known and the covariance matrix C_Φ in the characteristic space cannot be computed. The use of kernels bypasses the need to know

explicitly the function ϕ. The representation of the kernel otherwise reduces the nonlinear complex algorithms in **E** into simple linear formulations in **H**. Thus, we use the kernel trick (kernel trick), used primarily for the support vector machine (SVM) [34], [35], any algorithm in which the data appear as scalar products can be implicitly realized in **H** using kernel functions that allow the design of non-linear versions of linear algorithms.

Then, for all $x, x' \in \mathbb{R}^m$, and if $\mathbf{k}(.,.)$ is a positive definite kernel function on space that satisfies Mercer's theorem [36], the scalar product enters and is defined as follows:

$$\mathbf{k}(x, x') = \langle \phi(x), \phi(x') \rangle_H \tag{6}$$

We define $K \in \mathbb{R}^{N\times N}$ the kernel matrix whose elements $[K]_{ij}$ are determined from the equation(6) by:

$$\mathbf{K} = \chi\chi^T = \begin{bmatrix} \mathbf{k}(x_1, x_1) & \cdots & \mathbf{k}(x_1, x_N) \\ \vdots & \ddots & \vdots \\ \mathbf{k}(x_N, x_1) & \cdots & \mathbf{k}(x_N, x_N) \end{bmatrix} \tag{7}$$

The application of the kernel trick, to calculate the dot product $\langle \phi(x), \phi(x') \rangle_H$, can simplify the problem of decomposition into eigenvalues and eigenvectors of the covariance matrix C_Φ as follows, see [29] for a detailed explanation:

$$N\Lambda V = \mathbf{K}V \tag{8}$$

where $\Lambda = diag(\lambda_1 \ldots \lambda_j \ldots \lambda_N)$ is the diagonal matrix of eigenvalues λ_j ranked in descending order and $V = [\alpha_1 \ldots \alpha_j \ldots \alpha_N]$ is the matrix of their relative eigenvectors. Since it is essential to guarantee the normality of eigenvectors μ_j in the equation(4), as:

$$\langle \mu_j, \mu_j \rangle_H = 1;\ \mathrm{j} = 1 \ldots n \tag{9}$$

With n is the number of non-zero eigenvalues. Replacing equation (5) in equation (9) yields:

$$\begin{aligned} \langle \mu_j, \mu_j \rangle_H &= \sum_{i,\mathbf{k}}^{N} \alpha_{i,j}\alpha_{k,j} \langle \phi(x_i), \phi(x_k) \rangle_H \\ &= \sum_{i,\mathbf{k}}^{N} \alpha_{i,j}\alpha_{k,j} K_{i,k} \\ &= \langle \alpha_j, \mathbf{K}\alpha_j \rangle_H \\ &= \lambda_j \langle \alpha_j, \alpha_j \rangle_H \end{aligned} \tag{10}$$

Or $K_{i,k} = \mathbf{k}(x_i, x_k)$. The corresponding eigenvectors α_j must be normalized as follows:

$$\langle \alpha_j, \alpha_j \rangle_H = \|\alpha_j\|^2 = \frac{1}{\lambda_j};\quad \mathrm{j} = 1, \ldots, n \tag{11}$$

Then, the eigenvectors of the covariance matrix C_Φ construct a matrix μ_f such as:

$$\begin{aligned} \mu_f &= \left[\frac{\alpha_1}{\sqrt{\lambda_1}}\chi^T, \ldots, \frac{\alpha_\ell}{\sqrt{\lambda_\ell}}\chi^T, \frac{\alpha_{\ell+1}}{\sqrt{\lambda_{\ell+1}}}\chi^T, \ldots, \frac{\alpha_n}{\sqrt{\lambda_n}}\chi^T \right] \\ &= \Lambda^{-1/2} V \chi^T \end{aligned} \tag{12}$$

where ℓ the number of principal components is the most significant and sufficient to explain the variability of a process, the eigenvector matrices and eigenvalues can be decomposed into two sub-matrices as follows:

$$\mu_f = \left[\hat{\mu}_f\ \tilde{\mu}_f\right] \in \mathbb{R}^{N\times n};\ \Lambda = \begin{bmatrix} \hat{\Lambda} & 0 \\ 0 & \tilde{\Lambda} \end{bmatrix} \in \mathbb{R}^{n\times n} \tag{13}$$

$\hat{\mu}_f$ and $\hat{\Lambda}$ represent the matrices of the ℓ first eigenvectors and the ℓ first eigenvalues, respectively. $\tilde{\mu}_f$ and $\tilde{\Lambda}$ represent the matrices of the $(\mathrm{n} - \ell)$ last eigenvectors and the last $(\mathrm{n} - \ell)$ eigenvalues, respectively.

There are several kernel functions in the literature such as:

- Laplacian kernel:

$$k(x_i, x_j) = \exp(-\frac{\|x_i - x_j\|}{\sigma}) \tag{14}$$

- Gaussian kernel (radial basis function (RBF)):

$$k(x_i, x_j) = \exp(-\frac{\|x_i - x_j\|^2}{2\sigma^2}) \tag{15}$$

In equation (2), we assume that the transformed data $\phi(x_i)$ are implicitly centered $\sum_{i=1}^{N} \phi(x_i) = 0$. Generally, this is not the case, it leads to the normalization of the kernel matrix, where we replace **K** with the Gram matrix (G) as follows:

$$G = K - E_N K - K E_N + E_N K E_N \tag{16}$$

With $E_N = \frac{1}{N}\begin{pmatrix} 1 & \ldots & 1 \\ \vdots & \ddots & \vdots \\ 1 & \cdots & 1 \end{pmatrix} \in \mathbb{R}^{N\times N}$.

Once the KPCA model is obtained, the kernel vector $k(x_{test}) \in \mathbb{R}^{1\times N}$ of a test vector $x_{test} \in \mathbb{R}^m$ can be determined using the training data as $k\,(x_{test}) = [k\,(x_1, x_{test}) \cdots k\,(x_i, x_{test}) \cdots k\,(x_N, x_{test})]$. Before projecting the test vector into the feature space by the retained eigenvectors, the kernel vector $k(x_{test})$ must be centered. Then we have:

$$\bar{k}(x_{test}) = k(x_{test}) - E_1 K - k(x_{test}) E_N + E_1 K E_N \tag{17}$$

With $E_1 = \frac{1}{N}[1, \ldots, 1] \in \mathbb{R}^{1\times N}$

To compute the selected PC (ℓ), we apply the cumulative percent variance (CPV) [37]. The cumulative percent variance (CPV) can be expressed as:

$$CPV(\ell) = \frac{\sum_{j=1}^{\ell} \lambda_j}{\sum_{j=1}^{m} \lambda_j} 100\% \tag{18}$$

The number ℓ of selected principal components is chosen if the CPV is higher than 95%.

C. REVIEW OF RRKPCA METHOD

The main idea of the reduced rank KPCA method [38] is to remove the dependencies between the variables in the characteristic space and to keep a set of data reduced from the original one $X_r = [x_1, \ldots, x_i, \ldots, x_r]^T \in \mathbb{R}^{r\times m}$, where r is the number of observations retained. In order to identify the reference RR-KPCA model, the new most useful observation in terms of system information is saved in a reduced learning data matrix X_r. We consider that the system operates under normal conditions for N_0 moments. At each moment t, a new observation is collected, its kernel vector k_{x_t} is calculated and the kernel matrix is updated by adding a column and a line to the previous one, such as:

$$K_r^t = \begin{bmatrix} K_r^{t-1} & k_{x_t} \\ k_{x_t}^T & \mathbf{k}(x_t, x_t) \end{bmatrix} \in \mathbb{R}^{r\times r} \tag{19}$$

After the updating of the kernel matrix, we compute its rank. The rank value leads to two possibilities: in the first possibility the reduced data matrix increments by adding the new observation, if the kernel matrix has a full rank, this describes that the new observation is rich in information and defines the independence between the projected data in the feature space. In the second possibility, the reduced data matrix remains unchanged and we are returning the kernel matrix to its previous state, if the kernel matrix does not have a full rank, this describes that the new observation is not rich in information and causes the dependence between the data projected in the feature space.

Once all the observations have been evaluated, the reduced data matrix $X_r \in \mathbb{R}^{r\times m}$ is obtained and the reduced kernel matrix is constructed, as:

$$K_r = \begin{bmatrix} \mathbf{k}(x_1, x_1) & \cdots & \mathbf{k}(x_1, x_r) \\ \vdots & \ddots & \vdots \\ \mathbf{k}(x_r, x_1) & \cdots & \mathbf{k}(x_r, x_r) \end{bmatrix} \in \mathbb{R}^{r\times r} \tag{20}$$

Then, the reference model RR-KPCA (eigenvalues and eigenvectors) is estimated.

D. FAULT DETECTION INDEX

As in the linear PCA approach, the quadratic prediction error (SPE) is generally used for the detection of faults in the residual space using the Kernel PCA. However, the conventional KPCA method does not provide any data reconstruction approach in the characteristic space. Thus, the calculation of the SPE index is difficult. In [39] the authors proposed a simple expression for calculating the SPE index in the characteristic space at the moment k, which is represented as follows:

$$SPE(x_k) = \bar{k}(x_k, x_k) - \bar{k}^T(x_k)\, \hat{V}\, \Lambda^{-1}\, \hat{V}^T \bar{k}(x_k) \tag{21}$$

The process is considered in the normal situation at the instant k if:

$$SPE(x_k) < \delta_\alpha^2 \tag{22}$$

where δ_α^2 is the control limit of the SPE index, can be calculated using the chi2 distribution χ^2, given by:

$$\delta_\alpha^2 = g\chi_{h,\alpha}^2 \tag{23}$$

With h degrees of freedom and α is a confidence threshold with $(0 < \alpha < 1)$. The parameters g and h are determined as follows:

$$g = \frac{b}{2a} et \quad h = \frac{2a^2}{b} \tag{24}$$

where a and b represent the mean and variance of the index SPE.

III. SUGGESTED RBC-RRKPCA METHOD

A. PRINCIPLE

The idea of the RBC-RRKPCA method is to define the reconstruction of a defect detection index along the direction of a variable. Then, the variable with the largest amount of reconstruction is possibly the defective variable. In what follows, we will present the mathematical formulation of the proposed RBC-RRKPCA with the fault detection index SPE.

B. MATHEMATICAL FORMULATION

Consider $X_r \in \mathbb{R}^{r\times m}$ the reduced learning data matrix with r is the reduced data number and m the number of sensors, when a fault occurs in the sensor x_i, the faulty observation is $x \in \mathbb{R}^m$ and the fault direction is ξ_i. Thus, the measure reconstructed along the direction ξ_i is defined by:

$$z_i^r = x_r - \xi_i f_i \tag{25}$$

The objective of the reconstruction is to find the amplitude of default f_i such as the fault detection index of the reconstructed measurement $SPE\left(z_i^r\right)$ is minimized. It is therefore a question of solving the following optimization problem:

$$f_i = \arg\min SPE\,(x_r - \xi_i f_i) \tag{26}$$

In the case of RBC-PCA, the contribution based on the reconstruction of the variable x_i to the index SPE, RBC_i is the amount of reconstruction in the direction ξ_i, can be expressed as follows:

$$RBC_i = SPE\,(\xi_i f_i) \tag{27}$$

Nevertheless, [29] showed that the reconstruction contribution RBC of the index SPE cannot be calculated as shown in Equation (27) for the KPCA method. As a result, the RBC value can be calculated as the difference between the detection index of the faulty observation x and the detection index of the reconstructed observation z_i^r as follows:

$$RBC_i = SPE(z_i^r) - SPE(x_r) \tag{28}$$

Using equation(21), the detection index of the reconstructed observation z_i^r is defined by the following equation:

$$SPE(z_i^r) = \bar{k}(z_i^r, z_i^r) - \bar{k}^T(z_i^r)\, \hat{V}\, \Lambda^{-1}\, \hat{V}^T \bar{k}(z_i^r) \tag{29}$$

To calculate the RBC value in a direction ξ_i for the SPE index, where $\xi_i = [0\ 0\ 1\ \ldots\ 0]$ and the value 1 is placed in the i^{th} position. Therefore, it is about solving the optimization problem described by equation (26). Two optimization methods have been studied in [29]: the iterative method of fixed point [40], which calculates the value f_i directly and the Newton's optimization method, which not only allows to

calculate f_i, but also to find the convergence conditions of the optimization algorithm. Indeed, it has been shown that the algorithm fixed point is a special case of Newton's algorithm with large values of the kernel parameter σ,this condition ensures the minimization of the objective function and the convergence of the optimization algorithm. An important characteristic of the fixed point algorithm is that it does not imply the value σ explicitly, it means that the algorithm would converge with any value σ. According to equation, (29) the derivative of the index $SPE(z_i^r)$ with respect to f_i is given by:

$$\frac{\partial SPE(z_i^r)}{\partial f_i} = \frac{\partial \bar{k}(z_i^r, z_i^r)}{\partial f_i} - 2\bar{k}^T(z_i^r)\,\hat{V}_r\,\Lambda_r^{-1}\,\hat{V}_r^T\,\frac{\partial \bar{k}(z_i^r)}{\partial f_i} \quad (30)$$

With $\hat{V}_r$ and Λ_r are the first ℓ eigenvectors and eigenvalue of the reduced gram matrix, respectively. Thus, the derivative of $\bar{k}(z_i^r, z_i^r)$ with respect to f_i is defined by:

$$\frac{\partial \bar{k}(z_i^r, z_i^r)}{\partial f_i} = -2E_1^{rT}\frac{\partial k(z_i^r)}{\partial f_i} \quad (31)$$

With $\bar{k}(z_i^r, z_i^r) = 1 - 2\bar{k}^T(z_i^r)\mathrm{E}_1^r + \mathrm{E}_1^{rT}K\mathrm{E}_1^r, \mathrm{E}_1^r = \frac{1}{r}\begin{bmatrix}1 \cdots 1\end{bmatrix} \in \mathbb{R}^{1\times r}$

Using equation(17), the derivative of $\bar{k}(z_i^r)$ with respect to f_i can be expressed as follows:

$$\frac{\partial \bar{k}(z_i^r)}{\partial f_i} = F_r\frac{\partial k(z_i^r)}{\partial f_i} \quad (32)$$

With $F_r = I - E_r$ and $E_r = \frac{1}{r}\begin{bmatrix}1 \cdots 1\\ \vdots \ddots \vdots \\ 1 \cdots 1\end{bmatrix} \in \mathbb{R}^{r\times r}$

The substitution of equation (31) and (32) in (30) leads to the following of the derivative of the index $SPE(z_i^r)$ with respect to f_i:

$$\frac{\partial SPE(z_i^r)}{\partial f_i} = -2\left[E_1^r + F_r^T\hat{V}_r\,\Lambda_r^{-1}\,\hat{V}_r^T\bar{k}(z_i^r)\right]^T\frac{\partial k(z_i^r)}{\partial f_i} \quad (33)$$

The derivative of the vector $k(z_i^r)$ with respect to f_i is given by the following expression:

$$\frac{\partial k(z_i^r)}{\partial f_i} = \frac{\partial k(z_i^r)}{\partial z_i^r}\frac{\partial z_i^r}{\partial f_i} = \frac{2}{\sigma}(B_r\zeta_i - k(z_i^r)f_i) \quad (34)$$

With $B_r \begin{bmatrix}k(z_i^r, x_1^r)(x^r, x_1^r)^T\\ k(z_i^r, x_2^r)(x^r, x_r^r)^T\\ \vdots \\ k(z_i^r, x_r^r)(x^r, x_r^r)^T\end{bmatrix}$

Then the equation of the drift of the index $SPE(z_i^r)$ with respect to f_i (33) can be rewritten as follows:

$$\frac{\partial SPE(z_i^r)}{\partial f_i} = -\frac{4}{\sigma}\left[E_1^r + F_r^T\hat{V}_r\,\Lambda_r^{-1}\,\hat{V}_r^T\bar{k}(z_i^r)\right]^T \times \left(B_r\zeta_i - k\left(z_i^r\right)f_i\right) \quad (35)$$

To solve the optimization problem described by equation (26) and to find the amplitude f_i which minimizes the detection index associated with the reconstructed measure, we put the equation (35) to zero. The solution of f_i is given as follows:

$$f_i = \frac{\zeta_i^T B_r^T\left[E_1^r + F_r^T\hat{V}_r\,\Lambda_r^{-1}\hat{V}_r^T\bar{k}_r(z_i^r)\right]}{k_r^T(z_i)\left[E_1^r + F_r^T\hat{V}_r\,\Lambda_r^{-1}\hat{V}_r^T\bar{k}_r(z_i^r)\right]} \quad (36)$$

The flowchart summarizes the method of diagnosing defects by the proposed methodRBC-RRKPCA is presented in Figure 1.

IV. SIMULATION RESULTS

The effectiveness of this method has been proven and evaluated in terms of:

- Good detection rate (GDR) is defined as the ratio between the total number of defects detected and the total number of defective data
- False alarm rate (FAR): is calculated as the ratio between the total number of false alarms and the total number of data without fault
- Computing time (TE): the calculation time allocated for the execution of the algorithm of online detection.
- Average convergence time for fault location (TC): average convergence time of the optimization algorithm
- Good location rate (GLR): is defined as the ratio between the average value of RBC for the root cause of the change in the process and the total value of RBC for all directions

A. APPLICATION TO THE AIRLOR AIR QUALITY MONITORING NETWORK

The RBC-KPCA and RBC-RRKPCA techniques were used for diagnosis of defects on the air quality monitoring.

The air quality monitoring network (AIRLOR), operating in Lorraine, France. The AIRLOR contains 20 posts spread over several sites: rural, peri-rural and urban. Each post was used to acquire certain pollutants in the air, such as nitrogen oxides (NO and NO2), ozone (O3), carbon monoxide (CO), and sulfur dioxide (SO2). In this study, six stations are served for recording additional metrological parameters. The main objective is to detect the defects of the sensors, which measure the ozone concentration O3, the nitrogen oxides NO, and NO2. The phenomenon of photochemical pollution exhibits a non-linear dynamic behavior [4], [1] and [14]. The observation vector contains 18 controlled variables, corresponding respectively to the concentration of ozone, nitrogen oxide, and nitrogen dioxide of each station.

$$x(k) = \begin{bmatrix}\underbrace{v_1(k)\ v_2(k)\ v_3(k)}_{\text{station1}} & \cdots \underbrace{v_{10}(k)v_{11}(k)\ v_{12}(k)}_{\text{station4}}\\ \cdots \underbrace{v_{16}(k)\ v_{17}(k)\ v_{18}(k)}_{\text{station6}}\end{bmatrix}^T \quad (37)$$

400 observations were used in the training phase to construct the RBC-RRKPCA and RBC-KPCA reference model,

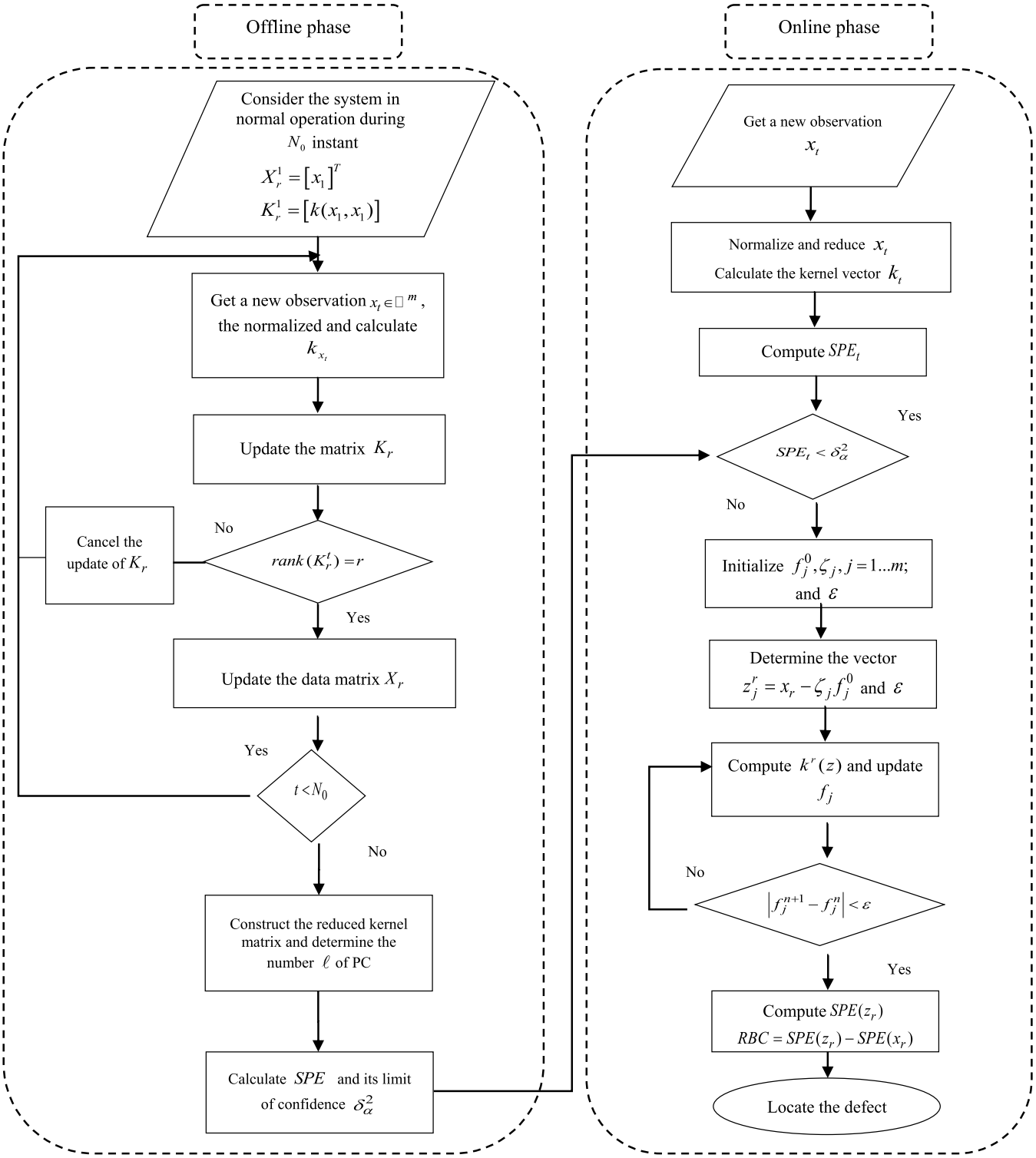

FIGURE 1. Flowchart for defect diagnosis by RBC-RRKPCA method.

besides, 1000 observations were used in the testing data phase. In this study, the RBF kernel was used and the kernel parameter is chosen using Tabu search algorithm [41]. The number of reduced observations selected using the proposed RBC-RRKPCA method is equal to 227, from 400 observations.

FIGURE 2. Air quality monitoring station.

To test the proposed fault detection algorithm, two faults with different amplitudes and time of appearance are introduced:

- Fault 1: is an additive fault by adding only 25% of the standard variation of (NO2) of station 3 between observations 350 and 650.
- Fault 2: is an additive fault by adding only 35% of the standard variation of (NO) of station 6 between observations 500 and 800.

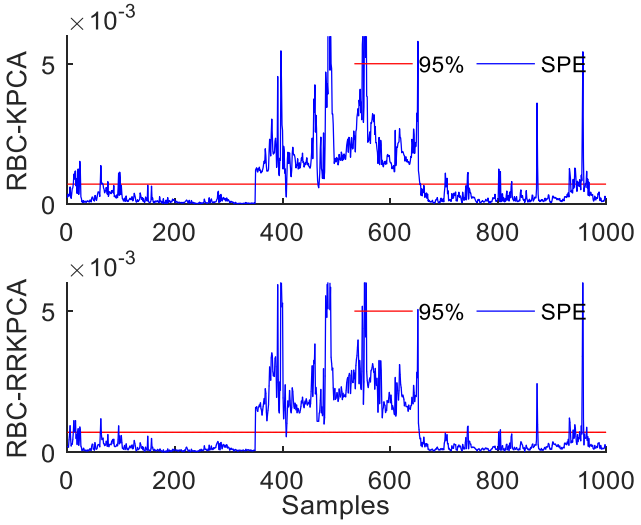

FIGURE 3. Fault detection results for Fault 1.

Figure 3 and Figure 4 present the evolution of the SPE index using RBC-KPCA and RBC-RRKPCA methods. As Fig. 3 and Fig. 4 show, the faults are correctly detected with the RBC-KPCA method, but with the presence of several false alarm for the 95% confidence limit. However, when using the proposed RBC-RRKPCA method, the FAR is decreased.

After detecting the fault, it is necessary to isolate its cause. Therefore, for each new observation, the RBC amount in the

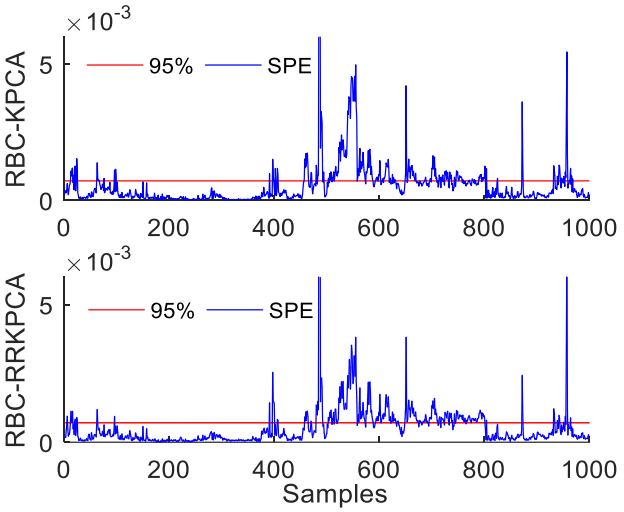

FIGURE 4. Fault detection results for Fault 2.

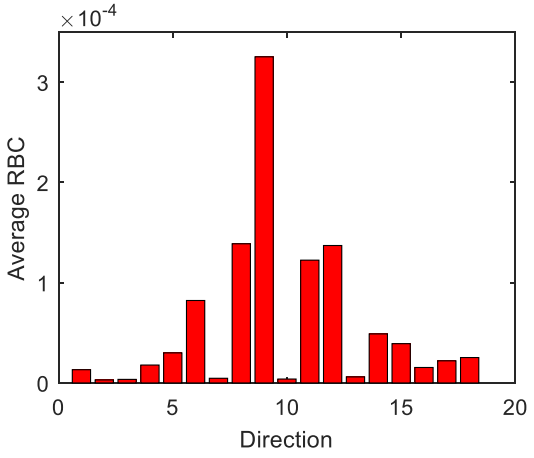

FIGURE 5. Fault localization using RBC-RRKPCA method for Fault 1.

18 directions (process variables) is calculated for the two faults using the RBC-KPCA and RBC-RRKPCA methods.

Figure 5 and Figure 6 shows the average RBC values using the RBC-RRKPCA method, calculated for each variable, for all defect samples and for the directions of the two analyzed faults.

As the Figure 5 shows, we can notice that the mean RBC values of the variable (NO2) of the 3rd station (direction 9) is the larger relative comparing to the values of the other variables, which means that it is the defective variable.

As shown in Figure 6, we can notice that the mean RBC values of the variable (NO) of the th station (direction 17) is the larger relative in contrast to the values of the other variables, which means that it is the defective variable.

Table 1 Table 2 represents the performances considered for the comparison between the two faults diagnosis methods. Note that the proposed method can significantly reduce the calculation time and the false alarm rate and guarantees a good detection rate especially in the case of second fault.

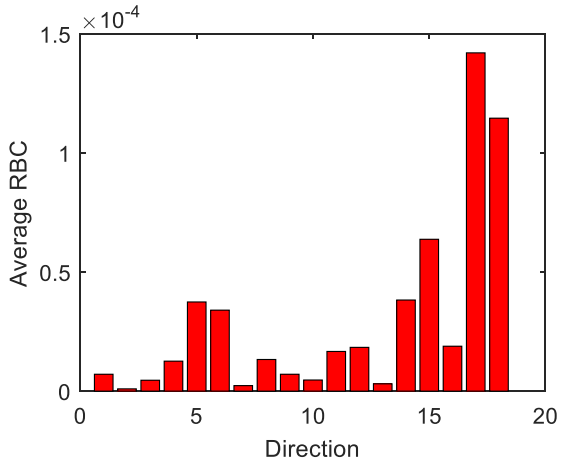

FIGURE 6. Fault localization using RBC-RRKPCA method for Fault 2.

TABLE 2. Fault diagnostic performances for RBC-KPCA and RBC-RRKPCA methods.

		RBC-KPCA	RBC-RRKPCA
Fault 1	FAR (%)	7.71	4.57
	GDR (%)	99	100
	TE(s)	1.66	0.97
	GLR (%)	100	100
	TC(s)	0.055	0.016
Fault 2	FAR (%)	10.71	7.85
	GDR (%)	64	85.33
	TE(s)	2.33	0.97
	GLR (%)	13.66	47.66
	TC(s)	0.037	0.0104

In addition, Table 2 shows that RBC-RRKPCA method guaranties a good localization with less average convergence time for fault location compared to conventional RBC-KPCA method.

B. APPLICATION TO TENNESSEE EASTMAN PROCESS (TEP)

To show the efficiency of the developed approach RBC-RRKPCA compared to RBC-KPCA [13] and RBC-RKPCA [42] methods, it is obligatory to test them on data of a strongly non-linear process. The Eastman chemical company created the TEP, which has been generally used to evaluate several fault diagnosis process. The TEP contains of five units, as presented in Figure 7a product extractor, a reactor, a liquid vapor separator, a condenser, and a compressor. TEP is largely detailed in the literature [7]. TEP is a nonlinear chemical reactor used to conduct chemical reactions. This process produces two main chemicals G and H and a by-product F from four reagents A, C, D, and E. The chemical reactions that the reactor produces are:

$$\begin{aligned} A(g) + C(g) + D(g) &\rightarrow G(liq) \\ A(g) + C(g) + E(g) &\rightarrow H(liq) \\ A(g) + E(g) &\rightarrow F(liq) \\ 3D(g) &\rightarrow 2F(liq) \end{aligned} \tag{38}$$

The TEP process contains in total 53 variables. These variables are subdivided into 12 manipulated variables and 41 measured variables. The 41 measured variables include 22 measured variables continuously and 19 measured variables in sampled. In this work, the observation vector contains the 22 measured variables in a continuous manner and 11 manipulated variables. Table 3 presents the measured and manipulated variables in the TEP process.

TABLE 3. Measured and manipulated variables that are monitored in the TEP.

Position	Variables	Description
Measured variables		
1	XMEAS(1)	A Feed (Stream 1)
2	XMEAS(2)	D Feed (Stream 2)
3	XMEAS(3)	E Feed (Stream 3)
4	XMEAS(4)	Total Feed (Stream 4)
5	XMEAS(5)	Recycle Flow (Stream 8)
6	XMEAS(6)	Reactor Feed Rate (Stream 6)
7	XMEAS(7)	Reactor Pressure
8	XMEAS(8)	Reactor Level
9	XMEAS(9)	Reactor Temperature
10	XMEAS(10)	Purge Rate (Stream 9)
11	XMEAS(11)	Product Sep Temp
12	XMEAS(12)	Product Sep Level
13	XMEAS(13)	Product Sep Pressure
14	XMEAS(14)	Product Sep Underflow (Stream 10)
15	XMEAS(15)	Stripper level
16	XMEAS(16)	Stripper Pressure
17	XMEAS(17)	Stripper Underflow (Stream 11)
18	XMEAS(18)	Stripper Temperature
19	XMEAS(19)	Stripper Steam Flow
20	XMEAS(20)	Compressor Work
21	XMEAS(21)	Reactor Cooling Water Temperature
22	XMEAS(22)	Separator Cooling Water Temperature
Manipulated Variables		
23	XMV(1)	D Feed Flow (Stream 2)
24	XMV(2)	E Feed (Stream 3)
25	XMV(3)	A Feed Flow (Stream 1)
26	XMV(4)	Total Feed Flow (Stream 4)
27	XMV(5)	Compressor Recycle Valve
28	XMV(6)	Purge Valve (Stream 9)
29	XMV(7)	Separator Pot Liquid Flow (Stream 10)
30	XMV(8)	Stripper Liquid Product Flow (Stream 11)
31	XMV(9)	Stripper Steam Valve
32	XMV(10)	Reactor Cooling Water Flow
33	XMV(11)	Condenser Cooling Water Flow

The observation vector comprises 33 measured and manipulated variables, which can be defined as follow:

$$x = [XMEAS(1) \ldots XMEAS(22)\ XMV(1) \ldots XMV(11)]^T \tag{39}$$

The TEP process presents several types of process faults, such as disturbances (bias faults), random variations, valve blockage, and unknown conditions. In this study, three types of TEP faults are analyzed: IDV (4), IDV (6), IDV (11), and IDV (14). These defects are indicated with their descriptions in the Table6and may affect one or more process variables; they have been introduced from observation 224.

A training set consists of 500 observations from the normal data that was used to build the KPCA, RKPCA [43]

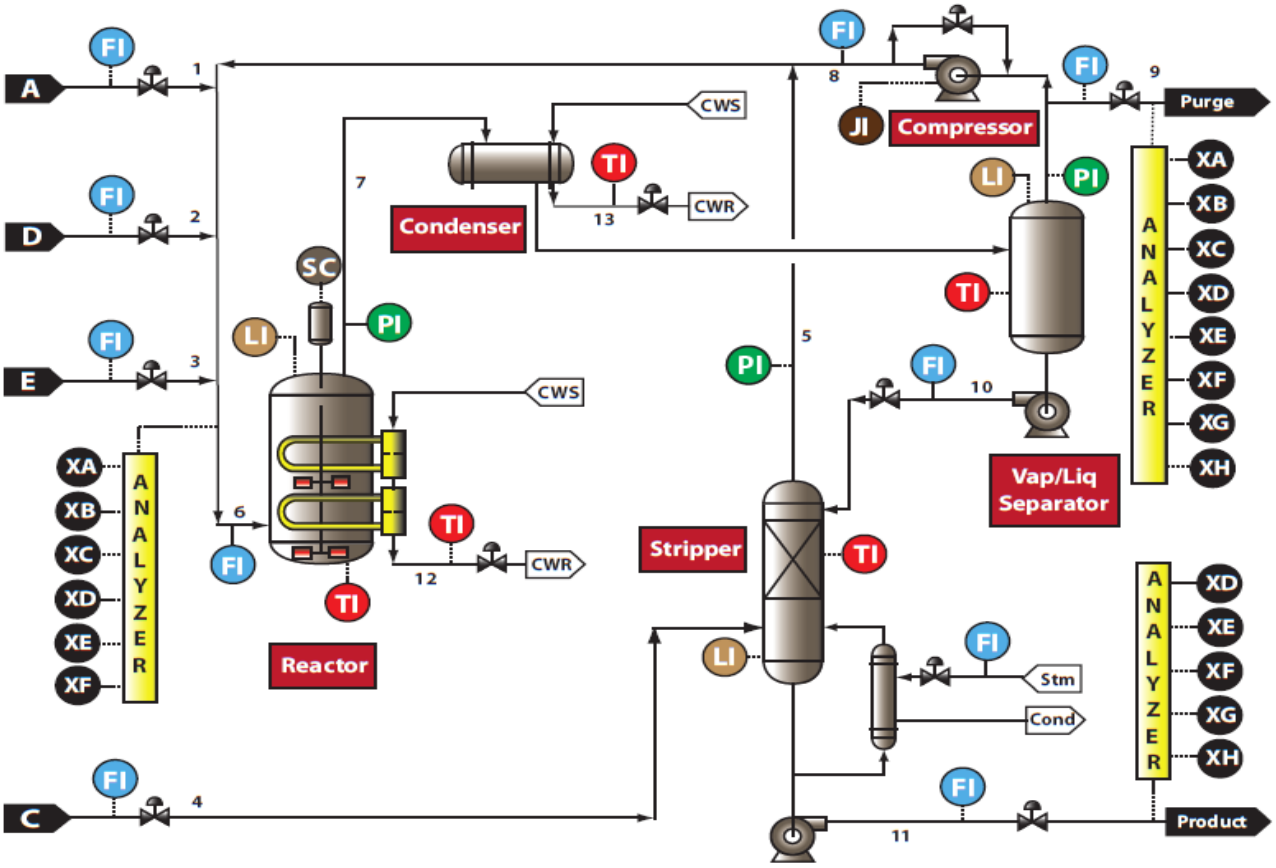

FIGURE 7. Diagram of the tennessee eastman process.

TABLE 4. Process faults for tennessee eastman process.

Fault number	Description	Type
IDV(4)	Reactor cooling water inlet temperature	Step
IDV(6)	A feed loss	Step
IDV(11)	Reactor cooling water inlet temperature	Random variation
IDV(14)	Reactor cooling water	Sticking

and RRKPCA reference models. Gaussian kernel function was used for linearization of data and the best value of the kernel parameter σ is selected using the Tabu-search algorithm [15], [44], [41]. The value of the kernel parameter is selected $\sigma = 7.6$ which guarantees less FAR, good GDR and smaller computing time. The reduced number of observations determined by the RKPCA [43] and the RRKPCA [38] methods is equal to 150 and 200 respectively.

Fig. 8 to Fig. 11 show the detection and the localization results of the different selected faults. The subfigures in the first column (8(a), 9(a), 10(a), and 11(a)) present the evolution of the SPE index using RBC-KPCA, RBC-RKPCA, and RBC-RRKPCA methods. As shown in the mentioned subfigures, the faults are correctly detected with the RBC-KPCA method, but with high false alarm rate in case of 95% confidence limit. However, when using our proposed method, the false alarm rate is decreased and lower than the RBC-KPCA method. The subfigures in the second column (8 (b), 9 (b), 10 (b), and 11 (b)) show the average RBC values using the RBC-RRKPCA method, calculated for each variable, for all the defect samples and for the directions of the four analyzed faults.

The first faulty scenario is a step change on the cooling water inlet temperature of the reactor IDV (4). Based on process knowledge, it is obvious that variation in the reactor cooling water will affect reactor temperature XMEAS (9) and the reactor cooling water temperature XMEAS (21). In this abnormal condition, the true root causes of the change in the reactor cooling water inlet temperature is the reactor cooling water flow XMV (10). Fig. 8b shows that the average value of RBCs for the monitoring variable XMV (10), direction 32 is the largest relative to the other variables, which means that it is the defective variable.

The second faulty scenario is IDV (6), which presents a sudden loss of flow in A feed. Because of this, feed A produces various changes that affect several variables such as A feed (stream 1), the total Feed (Stream 4), the reactor feed rate, and the reactor pressure. From the diagnosis results shown in Fig. 9b, we observe that the measured variable XMEAS (1) and the monitored variable XMV (3) have a

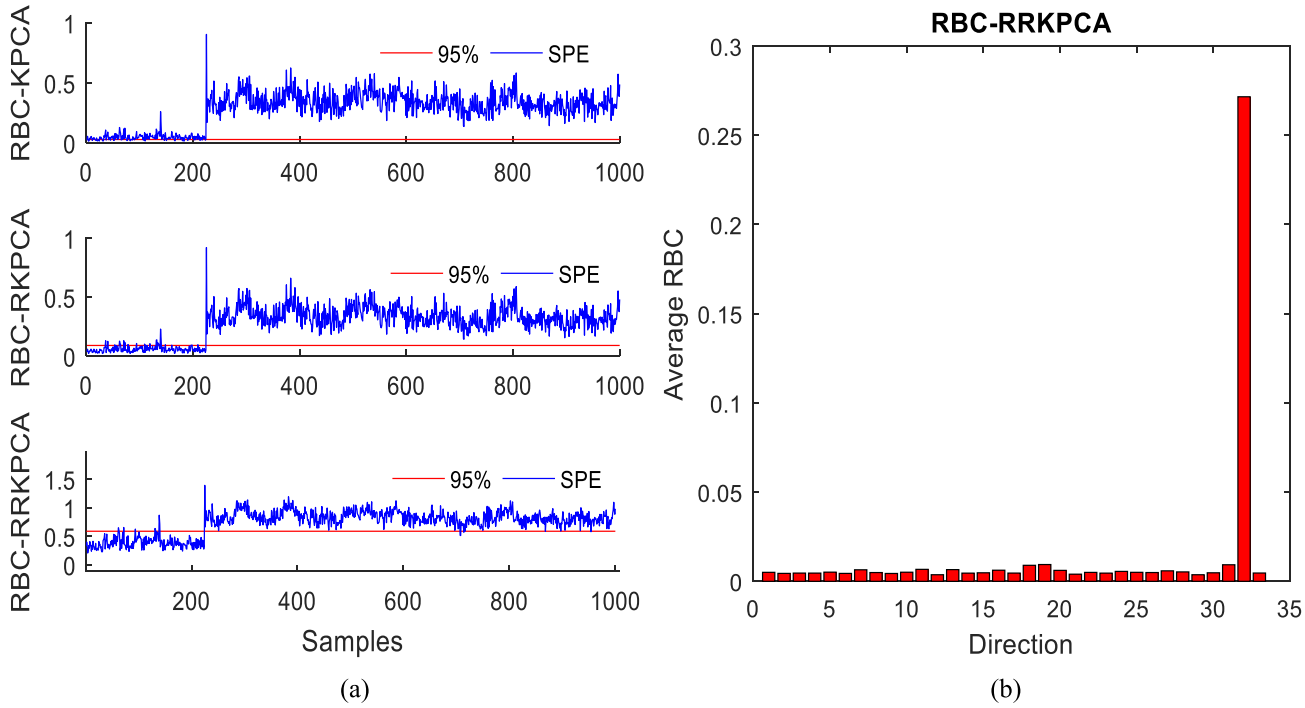

FIGURE 8. Fault detection and localization for Fault IDV (4).

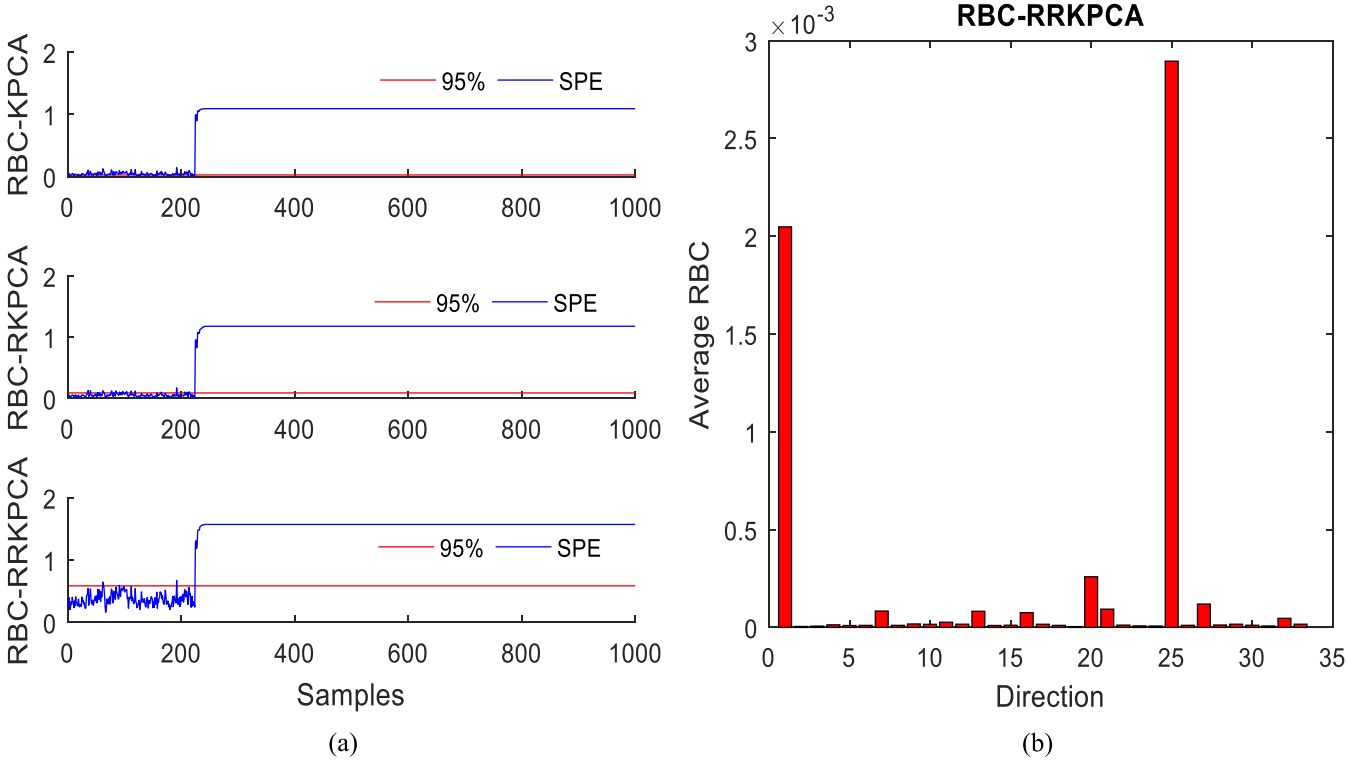

FIGURE 9. Fault detection and localization for Fault IDV (6).

largest contribution in this faulty condition. However, the variable XMV (3) (direction 25) has the highest contribution, with indicate that the monitored variable (A feed flow) is in faulty state.

In fault IDV (11) the reactor cooling water inlet temperature experiences a random variation, which increases the temperature in the reactor; the cause of this change is the increase in cooling water flow XMV (10). As Fig. 10(b)

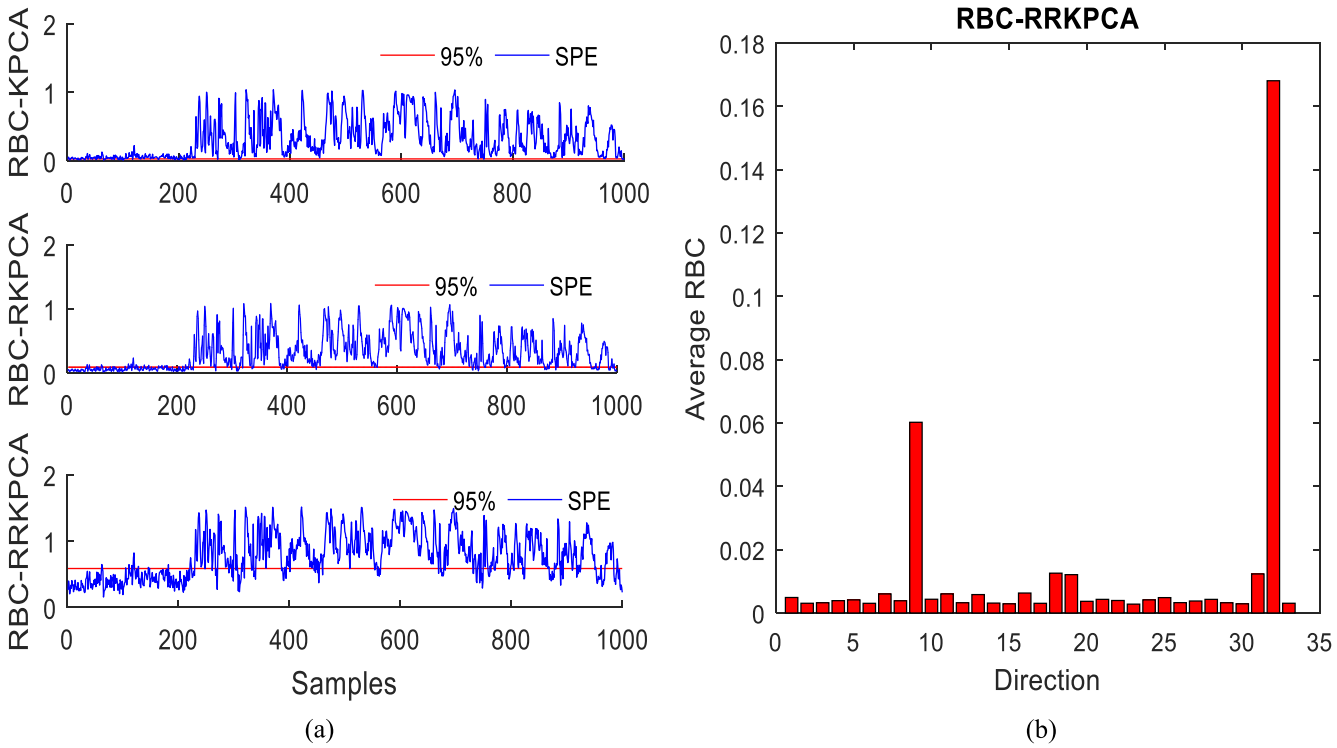

FIGURE 10. Fault detection and localization for Fault IDV (11).

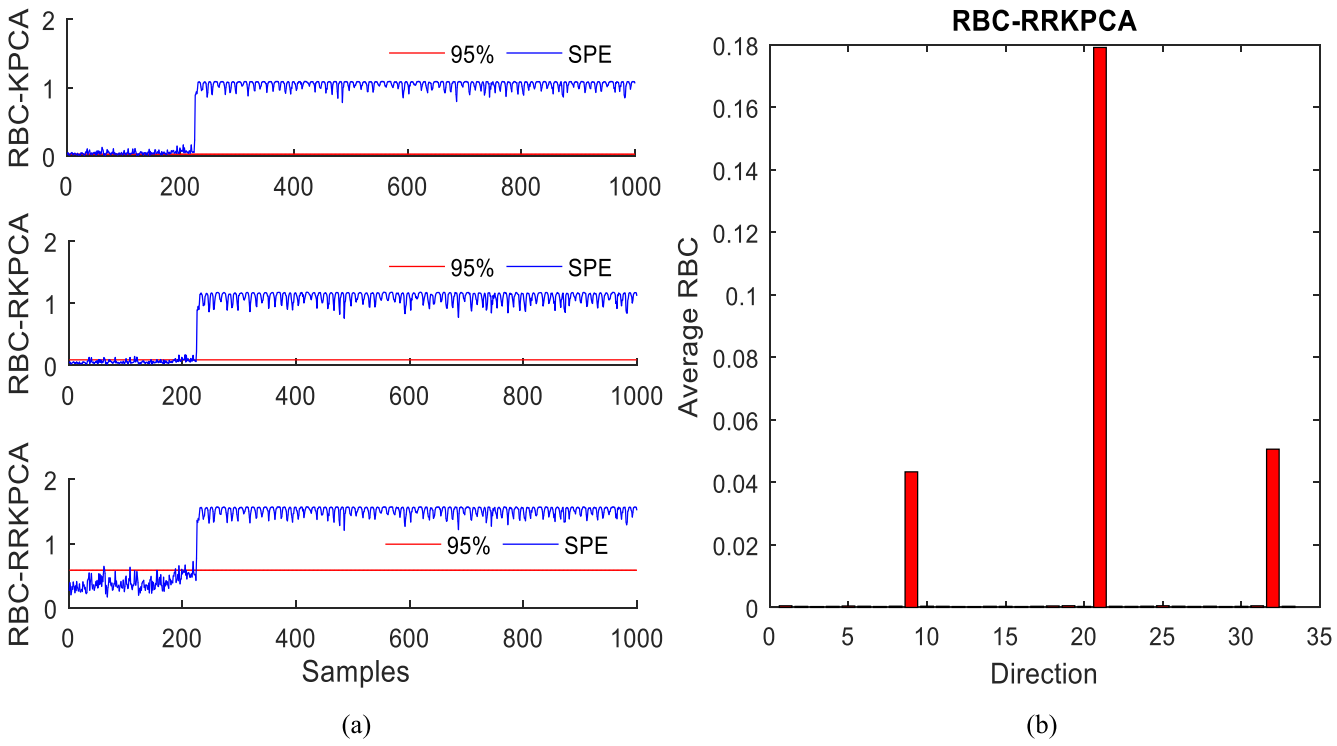

FIGURE 11. Fault detection and localization for Fault IDV (14).

shows, we can observe that the change in the cooling water flow is reflected in the diagnosis results, where the variable XMV (10) direction 32 has the highest average RBC values among all individual variables.

The fault IDV (14) presents the blockage of the reactor cooling water valve, this blockage influences both the reactor temperature (direction 9) and the reactor cooling water temperature (direction 21). As a result, this change causes an increment in the cooling water flow (direction 32) to regulate the reactor temperature. The blockage of the reactor cooling water valve is reflected in the diagnosis results, which can be seen in Fig. 11(b). The average RBCs for the reactor

temperature, the reactor cooling water flow, and the reactor cooling water temperature (directions: 9,32 and 21) are the largest relative to the values of the other variables. However, the average RBC value in the stored direction of IDV (14) (direction 21) is the largest value, indicating this value as the defective variable.

Table 5 represents the performance metric results for a comparison with the three methods of fault diagnosis. As shown in Table 5, our developed technique can significantly reduce the false alarm rate, the calculation time, and guaranties a good localization with less average convergence time for fault location.

TABLE 5. Fault diagnostic performances for RBC-KPCA, RBC-RKPCA and RBC-RRKPCA methods.

		RBC-KPCA	RBC-RKPCA	RBC-RRKPCA
IDV(4)	FAR (%)	79.01	11.60	3.57
	GDR (%)	100	100	99.22
	TE(s)	2.41	0.84	0.9
	GLR (%)	99.87	99.87	99.87
	TC(s)	0.213	0.065	0.022
IDV(6)	FAR (%)	75.44	12.5	1.78
	GDR (%)	100	100	100
	TE(s)	2.89	0.87	1.01
	GLR (%)	100	100	100
	TC(s)	0.09	0.0059	0.022
IDV(11)	FAR (%)	78.57	18.75	6.25
	GDR (%)	99.35	91.49	82.47
	TE(s)	2.61	0.67	0.82
	GLR (%)	100	99	99.22
	TC(s)	0.0069	0.0056	0.0058
IDV(14)	FAR (%)	79.01	14.28	3.57
	GDR (%)	100	100	100
	TE(s)	2.23	0.65	0.84
	GLR (%)	99.61	99.48	99.48
	TC(s)	0.133	0.054	0.0726

V. CONCLUSION

In this paper, the RRKPCA method based on RBC is developed. A remarkable case study of both the air quality monitoring network and the TEP system is provided to illustrate the method and to test its effectiveness. Results show that the proposed method can capture the inherent properties of each fault type and can improve the performance of RBC-KPCA.

Process-fault diagnosis is the method for guaranteeing the safety operation of a system in which fault detection and localization is a very important task. In other words, once a fault occurs, it should be quickly detected and located. However, the conventional RBC-KPCA method needs an important time for fault detection and localization due to the important size of the kernel matrix; therefore, it results in a high computing time to detect faults and a high false alarm rate. Meanwhile, the obtained results showed that the application of the RBC-RRKPCA method makes it possible to reduce the false alarm rate and the mean time of convergence, thus ensuring the rapid detection and localization of the defects. In other words, the proposed method can give us a good compromise between the different performances of fault detection and localization.

It should be noted that the proposed method cannot give the root cause of the fault once the fault has occurred, and it is unable to locate faults correctly in the case of fast dynamic systems, because the RRKPCA model is static.

Future work will be oriented toward locating the faults of dynamic nonlinear systems and integrating other methods in order to determine the root cause of the fault.

REFERENCES

[1] M.-F. Harkat, G. Mourot, and J. Ragot, "Multiple sensor fault detection and isolation of an air quality monitoring network using RBF-NLPCA model," *IFAC Proc. Volumes*, vol. 42, no. 8, pp. 828–833, 2009.

[2] Z. Yang and J. Wang, "A new air quality monitoring and early warning system: Air quality assessment and air pollutant concentration prediction," *Environ. Res.*, vol. 158, pp. 105–117, Oct. 2017.

[3] M. F. Harakat, "Détection et Localisation de Défauts par Analyse en Composantes Principales," M.S. thesis, Institut Nat. Polytechnique Lorraine, Vandœuvre-lès-Nancy, France, 2003.

[4] M.-F. Harkat, G. Mourot, and J. Ragot, "An improved PCA scheme for sensor FDI: Application to an air quality monitoring network," *J. Process Control*, vol. 16, no. 6, pp. 625–634, Jul. 2006.

[5] Y. Wang, D. Wu, and X. Yuan, "LDA-based deep transfer learning for fault diagnosis in industrial chemical processes," *Comput. Chem. Eng.*, vol. 140, Sep. 2020, Art. no. 106964.

[6] Y. Wang, H. Yang, X. Yuan, Y. A. W. Shardt, C. Yang, and W. Gui, "Deep learning for fault-relevant feature extraction and fault classification with stacked supervised auto-encoder," *J. Process Control*, vol. 92, pp. 79–89, Aug. 2020.

[7] M. Z. Sheriff, M. Mansouri, M. N. Karim, H. Nounou, and M. Nounou, "Fault detection using multiscale PCA-based moving window GLRT," *J. Process Control*, vol. 54, pp. 47–64, Jun. 2017.

[8] Q. Jiang, S. Yan, H. Cheng, and X. Yan, "Local-global modeling and distributed computing framework for nonlinear plant-wide process monitoring with industrial big data," *IEEE Trans. Neural Netw. Learn. Syst.*, early access, Apr. 21, 2020, doi: 10.1109/TNNLS.2020.2985223.

[9] A. Kulkarni, V. K. Jayaraman, and B. D. Kulkarni, "Knowledge incorporated support vector machines to detect faults in tennessee eastman process," *Comput. Chem. Eng.*, vol. 29, no. 10, pp. 2128–2133, Sep. 2005.

[10] Q. Jiang, X. Yan, H. Yi, and F. Gao, "Data-driven batch-end quality modeling and monitoring based on optimized sparse partial least squares," *IEEE Trans. Ind. Electron.*, vol. 67, no. 5, pp. 4098–4107, May 2020.

[11] Q. Jiang and X. Yan, "Parallel PCA–KPCA for nonlinear process monitoring," *Control Eng. Pract.*, vol. 80, pp. 17–25, Nov. 2018.

[12] A. Ragab, M. El-Koujok, M. Amazouz, and S. Yacout, "Fault detection and diagnosis in the tennessee eastman process using interpretable knowledge discovery," in *Proc. Annu. Rel. Maintainability Symp. (RAMS)*, 2017, pp. 1–7.

[13] C. F. Alcala and S. J. Qin, "Reconstruction-based contribution for process monitoring," *Automatica*, vol. 45, no. 7, pp. 1593–1600, Jul. 2009.

[14] M.-F. Harkat, M. Mansouri, M. Nounou, and H. Nounou, "Enhanced data validation strategy of air quality monitoring network," *Environ. Res.*, vol. 160, pp. 183–194, Jan. 2018.

[15] M. Said, K. B. Abdellafou, O. Taouali, and M. F. Harkat, "A new monitoring scheme of an air quality network based on the kernel method," *Int. J. Adv. Manuf. Technol.*, vol. 103, pp. 153–163, Mar. 2019.

[16] J. Gertler and T. McAvoy, "Principal component analysis and parity relations—A strong duality," in *Proc. IFAC Conf. SAFEPROCESS*, Hull, U.K., 1997, pp. 837–842.

[17] Y. Huang and J. Gertler, "Fault isolation by partial PCA and partial NLPCA," in *Proc. IFAC 14th Triennial World Congr.*, Beijing, China, 1999, pp. 545–550.
[18] M. Said, R. Fazai, K. B. Abdellafou, and O. Taouali, "Decentralized fault detection and isolation using bond graph and PCA methods," *Int. J. Adv. Manuf. Technol.*, vol. 99, nos. 1–4, pp. 517–529, Oct. 2018.
[19] R. Fazai, K. B. Abdellafou, M. Said, and O. Taouali, "Online fault detection and isolation of an AIR quality monitoring network based on machine learning and metaheuristic methods," *Int. J. Adv. Manuf. Technol.*, vol. 99, nos. 9–12, pp. 2789–2802, Dec. 2018.
[20] H. Lahdhiri, M. Said, K. B. Abdellafou, O. Taouali, and M. F. Harkat, "Supervised process monitoring and fault diagnosis based on machine learning methods," *Int. J. Adv. Manuf. Technol.*, vol. 102, pp. 1–17, Feb. 2019.
[21] B. Mnassri, E. M. El Adel, and M. Ouladsine, "Fault localization using principal component analysis based on a new contribution to the squared prediction error," in *Proc. 16th Medit. Conf. Control Automat.*, Jun. 2008, pp. 65–70.
[22] T. Kourti, "Application of latent variable methods to process control and multivariate statistical process control in industry," *Int. J. Adapt. Control Signal Process.*, vol. 19, no. 4, pp. 213–246, 2005.
[23] P. Miller, R. Swanson, and C. Heckler, "Contribution plots: A missing link in multivariate quality control," *Appl. Math. Comput. Sci.*, vol. 8, no. 4, pp. 775–792, 1998.
[24] S. J. Qin, "Statistical process monitoring: Basics and beyond," *J. Chemometrics*, vol. 17, nos. 8–9, pp. 480–502, 2003.
[25] C. Lee, S. W. Choi, J.-M. Lee, and I.-B. Lee, "Sensor fault identification in MSPM using reconstructed monitoring statistics," *Ind. Eng. Chem. Res.*, vol. 43, no. 15, pp. 4293–4304, Jul. 2004.
[26] H. H. Yue and S. J. Qin, "Reconstruction-based fault identification using a combined index," *Ind. Eng. Chem. Res.*, vol. 40, no. 20, pp. 4403–4414, Oct. 2001.
[27] G. A. Cherry and S. J. Qin, "Multiblock principal component analysis based on a combined index for semiconductor fault detection and diagnosis," *IEEE Trans. Semicond. Manuf.*, vol. 19, no. 2, pp. 159–172, May 2006.
[28] C. F. Alcala and S. J. Qin, "Reconstruction-based contribution for process monitoring with kernel principal component analysis," *Ind. Eng. Chem. Res.*, vol. 49, no. 17, pp. 7849–7857, Sep. 2010.
[29] C. F. Alcala, "Fault diagnosis with reconstruction based contributions for statistical process monitoring," M.S. thesis, L'école USC Univ. California Sud, Los Angeles, CA, USA, 2011.
[30] B. Schölkopf, A. Smola, and K.-R. Müller, "Nonlinear component analysis as a kernel eigenvalue problem," *Neural Comput.*, vol. 10, no. 5, pp. 1299–1319, Jul. 1998.
[31] S. Neffati, K. B. Abdellafou, O. Taouali, and K. Bouzrara, "A new bio-CAD system based on the optimized KPCA for relevant feature selection," *Int. J. Adv. Manuf. Technol.*, vol. 102, nos. 1–4, pp. 1023–1034, May 2019.
[32] D. Dong and T. J. McAvoy, "Nonlinear principal component analysis—Based on principal curves and neural networks," *Comput. Chem. Eng.*, vol. 16, pp. 313–328, Jan. 1992.
[33] F. Jia, E. B. Martin, and A. J. Morris, "Non-linear principal components analysis for process fault detection," *Comput. Chem. Eng.*, vol. 22, pp. 851–854, Mar. 1998.
[34] V. N. Vapnik, *Statistical Learning Theory*. New York, NY, USA: Wiley, 1998.
[35] H. Lahdhiri, O. Taouali, I. Elaissi, I. Jaffel, M. F. Harakat, and H. Messaoud, "A new fault detection index based on Mahalanobis distance and kernel method," *Int. J. Adv. Manuf. Technol.*, vol. 91, nos. 5–8, pp. 2799–2809, Jul. 2017.
[36] J. Mercer, "Functions of positive and negative type and their connection with the theory of integral equations," *Philos. Trans. Roy. Soc. London A, Math. Phys. Sci.*, vol. 209, pp. 415–446, Apr. 1909.
[37] S. Valle, W. Li, and S. J. Qin, "Selection of the number of principal components: The variance of the reconstruction error criterion with a comparison to other methods," *Ind. Eng. Chem. Res.*, vol. 38, no. 11, pp. 4389–4401, Nov. 1999.
[38] H. Lahdhiri, I. Elaissi, O. Taouali, M. F. Harakat, and H. Messaoud, "Nonlinear process monitoring based on new reduced rank-KPCA method," *Stochastic Environ. Res. Risk Assessment*, vol. 32, no. 6, pp. 1833–1848, Jun. 2018.
[39] S. W. Choi, C. Lee, J.-M. Lee, J. H. Park, and I.-B. Lee, "Fault detection and identification of nonlinear processes based on kernel PCA," *Chemometric Intell. Lab. Syst.*, vol. 75, no. 1, pp. 55–67, Jan. 2005.
[40] B. Schölkopf, S. Mika, A. Smola, G. Rätsch, and K. Müller, "Kernel PCA pattern reconstruction via approximate pre-images," in *Proc. ICANN*, vol. 98. London, U.K.: Springer, 1998, pp. 147–152.
[41] H. Lahdhiri, K. B. Abdellafou, O. Taouali, M. Mansouri, and O. Korbaa, "New online kernel method with the tabu search algorithm for process monitoring," *Trans. Inst. Meas. Control*, vol. 41, no. 10, pp. 2687–2698, Jun. 2019.
[42] I. Jaffel, R. Fezai, O. Taouali, M. F. Harkat, and H. Messaoud, "Fault detection localization and reconstruction in nonlinear system using RKPCA method and RBC," in *Proc. Int. Conf. Control, Automat. Diagnosis (ICCAD)*, Jan. 2017, pp. 487–492.
[43] O. Taouali, I. Jaffel, H. Lahdhiri, M. F. Harkat, and H. Messaoud, "New fault detection method based on reduced kernel principal component analysis (RKPCA)," *Int. J. Adv. Manuf. Technol.*, vol. 85, nos. 5–8, pp. 1547–1552, Jul. 2016.
[44] K. B. Abdellafou, H. Hadda, and O. Korbaa, "An improved tabu search meta-heuristic approach for solving scheduling problem with non-availability constraints," *Arabian J. Sci. Eng.*, vol. 44, no. 4, pp. 3369–3379, Apr. 2019.

HAJER LAHDHIRI was born in Ksar Hellal, Monastir, Tunisia, in 1989. She received the engineering and Ph.D. degrees in electrical from the National Engineering School of Monastir, Tunisia, in 2013 and 2018, respectively. Her work focuses on the use of applied mathematics and statistics concepts to develop statistical data and model-driven techniques and algorithms for modeling, fault detection, and monitoring.

AHAMED ALJUHANI received the bachelor's degree in computer and information systems from Fahad Bin Sultan University, Tabuk, Saudi Arabia, in 2010, and the M.S. degree in computer science from the University of Colorado Denver, Denver, USA, in 2013, and the Ph.D. degree in computer science from The Catholic University of America, Washington D.C., USA, in 2020. He is currently an Assistant Professor and the Chair of the Computer Engineering Department, College of Computing and Information Technology, University of Tabuk, Saudi Arabia.

KHAOULA BEN ABDELLAFOU received the bachelor's degree in computer science from the Faculty of Science, Monastir, Tunisia, in 2011, the master's degree in computer science, in 2013, and the Ph.D. degree in computer science from ISITCom, University of Sousse. She is currently working as an Assistant Professor with the Faculty of Computers and Information Technology, University of Tabuk, Saudi Arabia. Her research interests include parallel computing, optimization, heuristic and metaheuristic, machine learning, pattern recognition, and image processing.

OKBA TAOUALI received the engineering degree in electrical engineering from the National Engineering School of Monastir (ENIM), Monastir University, Tunisia, in 2005, with a focus on computer engineering, the Ph.D. degree from ENIM, in 2010, and the H.D.R. degree from Monastir University, in 2016. He worked as an Associate Professor in electrical and computer engineering with ENIM. He is currently working as an Associate Professor with the Faculty of Computers and Information Technology, University of Tabuk, Saudi Arabia. His research interests include machine learning, kernel methods, fault diagnosis, process modeling and monitoring, multivariate statistical approaches, pattern recognition, and image processing.